

# Neuronal Blockade of Thyroid Hormone Signaling Increases Sensitivity to Diet-Induced Obesity in Adult Male Mice

Eva Rial-Pensado,<sup>1</sup> Laurence Canaple,<sup>2,†</sup> Romain Guyot,<sup>2,‡</sup> Christoffer Clemmensen,<sup>3,†</sup> Joëlle Wiersema,<sup>4</sup> Shijia Wu,<sup>2</sup> Sabine Richard,<sup>2</sup> Anita Boelen,<sup>4</sup> Timo D. Müller,<sup>3,5</sup> Miguel López,<sup>1</sup> Frédéric Flamant,<sup>2</sup> and Karine Gauthier<sup>2</sup>

<sup>1</sup>NeuroObesity Group, Department of Physiology, CiMUS, University of Santiago de Compostela, Instituto de Investigación Sanitaria & CIBER de la Fisiología de la Obesidad y la Nutrición (CIBEROBN), Santiago de Compostela 15782, Spain

<sup>2</sup>Univ Lyon, ENS de Lyon, INRAE, CNRS, Institut de Génomique Fonctionnelle de Lyon, Lyon 69364, France

<sup>3</sup>Institute for Diabetes and Obesity, Helmholtz Diabetes Center at Helmholtz Zentrum München, German Research Center for Environmental Health, Neuherberg 85764, Germany

<sup>4</sup>Department of Clinical Chemistry, Endocrine Laboratory, Amsterdam Gastroenterology & Metabolism, Amsterdam UMC, University of Amsterdam, Amsterdam 1105AZ, The Netherlands

<sup>5</sup>German Center for Diabetes Research (DZD), Neuherberg 85764, Germany

**Correspondence:** Karine Gauthier, PhD, Univ Lyon, ENS de Lyon, INRAE, CNRS, Institut de Génomique Fonctionnelle de Lyon, 32-34 Avenue Tony Garnier, 69007 Lyon, France. Email: [karine.gauthier@ens-lyon.fr](mailto:karine.gauthier@ens-lyon.fr).

<sup>†</sup>Present address: Univ Lyon, ENS de Lyon, Inserm US8, CNRS UMS3444, SFR Biosciences, 50 Avenue Tony Garnier, Lyon F-69007, France.

<sup>‡</sup>Present address: Novo Nordisk Foundation Center for Basic Metabolic Research, Faculty of Health and Medical Sciences, University of Copenhagen, Copenhagen, Denmark.

## Abstract

Thyroid hormone increases energy expenditure. Its action is mediated by TR, nuclear receptors present in peripheral tissues and in the central nervous system, particularly in hypothalamic neurons. Here, we address the importance of thyroid hormone signaling in neurons, in general for the regulation of energy expenditure.

We generated mice devoid of functional TR in neurons using the Cre/LoxP system. In hypothalamus, which is the center for metabolic regulation, mutations were present in 20% to 42% of the neurons.

Phenotyping was performed under physiological conditions that trigger adaptive thermogenesis: cold and high-fat diet (HFD) feeding. Mutant mice displayed impaired thermogenic potential in brown and inguinal white adipose tissues and were more prone to diet-induced obesity. They showed a decreased energy expenditure on chow diet and gained more weight on HFD. This higher sensitivity to obesity disappeared at thermoneutrality. Concomitantly, the AMPK pathway was activated in the ventromedial hypothalamus of the mutants as compared with the controls. In agreement, sympathetic nervous system (SNS) output, visualized by tyrosine hydroxylase expression, was lower in the brown adipose tissue of the mutants. In contrast, absence of TR signaling in the mutants did not affect their ability to respond to cold exposure.

This study provides the first genetic evidence that thyroid hormone signaling exerts a significant influence in neurons to stimulate energy expenditure in some physiological context of adaptive thermogenesis. TR function in neurons to limit weight gain in response to HFD and this effect is associated with a potentiation of SNS output.

**Key Words:** thyroid hormone, adaptive thermogenesis, cold exposure, diet-induced obesity, neurons, brown adipose tissue, sympathetic nervous system (SNS)

**Abbreviations:** AMPK, AMP-activated protein kinase; BAT, brown adipose tissue; CTRL, control mice; D2, type 2 deiodinase; DIO, diet-induced obesity; EE, energy expenditure; HFD, high-fat diet; ICV, intracerebroventricular; iWAT, inguinal WAT; LA, locomotive activity; NE, norepinephrine; NTRKO, mutant mice (*Cre3<sup>tg/+</sup>xThra<sup>AM1/+</sup>Thrb<sup>lox/lox</sup>*); PTU, propylthiouracil; ROI, region of interest; RT-qPCR, quantitative reverse transcription–polymerase chain reaction; SNS, sympathetic nervous system; T3, triiodothyronine; T4, thyroxine; TH, thyroid hormones; UCP1, uncoupling protein 1; VMH, ventromedial hypothalamus; WAT, white adipose tissue; WT, wild-type.

As obesity and associated metabolic disorders became pandemic (1), the metabolic activities of thyroid hormone (3,3',5-triiodo-L-thyronine, or T3), the active metabolite of thyroxine (T4) gained renewed interest. Indeed, in humans, hyperthyroidism often results in weight loss, whereas hypothyroidism tends to favor weight gain. Most importantly, exogenous T3 increases energy expenditure (EE) both in humans and rodents (2). As a result, an excess of T3 induces weight loss despite an increase in food intake (3).

T3 can increase EE either directly or indirectly. Its direct metabolic action takes place in brown adipose tissue (BAT), white adipose tissue (WAT), muscle and liver, where it stimulates the mitochondrial metabolism. In BAT, T4 can be deiodinated to produce T3. This local production of T3 triggers the expression of UCP1, the protein responsible for the uncoupling between oxidative phosphorylation and ATP production, which has an important function in thermogenesis (4, 5). After hormonal stimulation, several enzymes involved

in lipid synthesis and calories production are also induced in BAT (6), and EE increases in muscle (7, 8). T3 also triggers WAT browning, that is, the conversion of some white adipocytes into thermogenic adipocytes producing UCP1 (9).

In addition to its direct influence on peripheral tissues, T3 is also involved in the central control of adaptive thermogenesis (10, 11), a process that is activated to face 2 types of external stress: cold exposure and excess of food intake (12). Perception of cold exposure by skin receptors is sensed by the hypothalamus and results in an increased activity of the sympathetic nervous system (SNS). The subsequent stimulation of adrenergic synapses in adipose tissues triggers immediate BAT thermogenesis, and late browning of WAT (13, 14). SNS stimulation leads to both UCP1-dependent and UCP1-independent thermogenesis in BAT (15-17) and muscle (18). How a high-fat diet (HFD) provokes a thermogenic response is less documented. While the involvement of the SNS in this response is well established, the contribution of BAT seems limited (19, 20). Importantly, stimulation of BAT via the SNS results in increased expression of the *Dio2* gene and a concomitant increase in type 2 deiodinase (D2) activity (21). The resulting local conversion of T4 into T3 contributes to an increased thermogenic activity. *Dio2* knock-out mice are more sensitive to cold (20) and more prone to diet-induced obesity (DIO) (22).

Hypothalamic glial cells including astrocytes and tanycytes contain D2, which allows a local conversion of T4 into T3 (23). The fact that this local conversion is involved in adaptive thermogenesis is supported by experiments that show that an intrahypothalamic excess of T3 is sufficient to stimulate BAT activity (10). As all cell types in the hypothalamus express the nuclear receptors of T3, either TR $\alpha$ 1 encoded by the *Thra* gene, or TR $\beta$ 1/2 encoded by *Thrb* (24), they all have the capacity to respond to a local increase in T3. However, the link between the intrahypothalamic T3 concentration and the increase in sympathetic tone remains unclear. Elevation of intrahypothalamic T3 concentration is characterized by rapid activation of the AMP-activated protein kinase (AMPK)-ER stress-JNK1 pathway in neurons (10, 25). Although their T3 response is not documented, neuronal populations located in other areas of the brain, notably the brainstem, also participate in EE (26).

We address here the importance of T3 signaling in neurons for the regulation of EE under thermogenic stresses. To this end, we used the Cre/loxP methodology to produce a mouse model in which the T3 response is selectively eliminated from a significant fraction of neurons, notably in 20% to 42% of the neurons in the hypothalamus depending on the nucleus. We evaluated the ability of these mice to face thermogenic stress. Mice were exposed either to an intense cold or fed for several months with an HFD. Mutant mice display an intact thermogenic response after exposure to cold at 4 °C but were more prone to DIO. The decrease in SNS tone in the mutants mimics what was observed after virogenetic inhibition of TR signaling in the hypothalamus and mirrors the increase triggered by intracerebroventricular (ICV) T3 administration (10, 25). Overall, our data show that endogenous T3 signaling exerts a significant influence on neurons involved in the regulation of energy metabolism.

## Methods

### Chemicals

Triiodothyronine (T3) and thyroxine (T4) were from Sigma-Aldrich (l'Isle D'Abeau, France).

## Mice Lines

Mutant mice were obtained by crosses in the C57BL6/J genetic background to introduce different recombinant alleles. *Thra*<sup>AMI</sup> allows the production of the TR $\alpha$ 1<sup>L400R</sup> mutant, which has dominant-negative properties, after Cre/loxP-mediated excision of a stop cassette (27). Despite the persistence of an intact *Thra* allele in *Cre3*<sup>Tg/+</sup>*xThra*<sup>AMI/+</sup> mice, the dominant negative action of TR $\alpha$ 1<sup>L400R</sup> eliminates the capacity of cells expressing *Thra* to respond to T3. *Thrb*<sup>lox</sup> has 2 tandem-arranged loxP sequences, allowing Cre-mediated excision of exon 3, which encodes the DNA binding domain of the TR $\beta$ 1/TR $\beta$ 2 receptor, resulting in a frameshift and a loss of function (28). *Cre3*<sup>Tg</sup> (29) is a randomly integrated transgene that drives the expression of the Cre recombinase expression in neurons of the central nervous system, but also the peripheral nervous system. The fraction of neurons with active Cre differs in the different areas and is markedly higher in hypothalamus as compared to other areas of the brain (30). Cre activity was not detected in astrocytes or non-neuronal cell types (29, 30). We previously verified this specific neuronal expression using the *rosa* YFP reporter line (31). Furthermore, in the present study, using the *ROSA tdTomato* reporter transgene (32), we verified the absence of recombination activity outside the nervous system, except for a small fraction of cardiomyocytes (Supplementary Fig. S1) (33). *Cre3*<sup>Tg/+</sup>*xROSAtdTomato* mice were also used to highlight with red fluorescence the hypothalamic cells in which Cre-mediated recombination occurred and compare the percentage of neurons that present Cre activity in the different part of the hypothalamus (Supplementary Fig. S2 (33)). Mice with the *Cre3*<sup>Tg/+</sup>*xThra*<sup>AMI/+</sup>*Thrb*<sup>lox/lox</sup> genotype are called Neuron TRKO (NTRKO). *Thra*<sup>AMI/+</sup>*Thrb*<sup>lox/lox</sup> littermates were used as controls (CTRL).

All experiments were carried out in accordance with the European Community Council Directive of September 22, 2010 (2010/63/EU) regarding the protection of animals used for experimental and other scientific purposes. The research project was approved in the different institutions. In Lyon, it was approved by a local animal care and use committee (C2EA015) and subsequently authorized by the French Ministry of Research, in Santiago by the USC Ethics Committee (Project ID 15010/14/006) and in München by the Animal Ethics Committee of the government of Upper Bavaria, Germany. A total of 180 mice have been used for this study.

## Animal Procedures and Preparation of Tissue Samples

### Housing

Mice were fed an ad libitum LASQC Rod16 R diet (Altromin, Germany) (16.9% proteins; 4.3% fat and 79.2% carbohydrates, hereafter called CHOW), housed 2 per cage when possible, or otherwise mentioned, at 23 °C, under a 7:30 AM: 8:30 PM light/dark cycle. 3- to 5-month-old male mice were used for experiments.

### Cold exposure and thermography

The cold response was assessed in mice implanted with IPTT-300 transponders (Plexx BV, The Netherlands) by exposing them to 4 °C for 58 hours. Infrared thermography was performed at different time points in awake and free running animals. To capture static dorsal thermographic images,

thermal videos of 2 minutes duration each were recorded using an infrared camera (FLiR Systems, Inc.). Thermal images were analyzed using the FLiR Research IR program. Regions of interest (ROI) were drawn so that each type of ROI was overlaid on all thermal images at once. This allowed for identical sizing of each type of ROI across all mice. An ROI on the basis of the tail served as the temperature control, while an ROI surrounding the interscapular region served to evaluate BAT thermogenesis. The temperature difference between these 2 ROI was calculated and used as a proxy of BAT activation. For each time point, 4 images per mouse were analyzed. Four mice per genotype were included in the experiment.

When mentioned, the experiments were performed at thermoneutrality in thermoregulated chambers.

### Induction of hypo/hyperthyroidism

T3 deficiency in adult animals was induced as previously described with a diet containing PTU (propylthiouracil) (Harlan Teklad TD95125, Madison, WI) (25.3% protein, 10% fat, 64.8% carbohydrates and 0.15% PTU) and followed or not by thyroid hormones (TH) (mix of T4 and T3) daily injections (34) for 5 consecutive days. Mice ate between 3.75 and 5.25 mg/day of PTU (2.5 and 3.5 g of diet per day). Serum concentrations of free T3 and free T4 were measured as described in "Plasma Biochemistry" and were approximately 1 pmol/l for both free T3 and free T4 in all genotypes in the PTU-treated groups and, respectively, above 50 pmol/l and 100 pmol/l (the maximum concentrations detectable by the assay) in all genotypes in the PTU/TH treated groups. As expected, PTU leads to hypothyroidism whereas TH injection leads to hyperthyroidism.

### HFD feeding

The response to HFD (Research Diets, New Brunswick, USA, D12331) (16.4% proteins; 58% fat and 25.5% carbohydrates) was evaluated after acute feeding periods (3.5 days) or prolonged feeding periods (3 to 7 months).

### Indirect calorimetry

A calorimetric system (LabMaster; TSE Systems; Bad Homburg, Germany) was used to assess EE and locomotor activity. Animals were placed 1 per cage with controlled conditions of air and temperature (24 °C). Mice were in adaptation for a week before starting the measurements. After calibrating the system with the reference gases (20.9% O<sub>2</sub>, 0.05% CO<sub>2</sub>, and 79.05% N<sub>2</sub>), the metabolic rate was measured for 48 hours as previously described (35). EE, RQ (VCO<sub>2</sub>/VO<sub>2</sub>) and Locomotive Activity (LA) were recorded every 30 minutes. Mice were injected subcutaneously with 1 mg/kg of norepinephrine bitartrate salt monohydrate (Sigma, Germany) to analyze the response to norepinephrine (NE). The O<sub>2</sub> consumption was then measured for another 120-160 minutes every 10 minutes.

### Tissue sampling

At the end of the experiments, mice were anesthetized at 2 PM (intraperitoneal injection of a mixture of xylazine and ketamine) to collect blood from the inferior vena cava in heparin coated tubes. Plasma was obtained after centrifugation at 3500 rpm for 15 minutes. Tissues were dissected and snap-frozen in liquid nitrogen and stored at -80 °C for later RNA preparation or fixed in zinc

formal Fixx (ThermoFisher Scientific, Waltham, MA, USA) for histology and immunohistochemistry.

For neuroanatomy experiments, the thorax was opened and each mouse was perfused with 4% paraformaldehyde in 0.1M phosphate buffer at room temperature and the brain processed as previously described (30).

### RNA Extraction and Expression Analyses by Relative Quantitative Reverse Transcription-Polymerase Chain Reaction

Total RNA was prepared using the TRI Reagent (ThermoFisher Scientific) protocol followed by a RNase free DNase treatment (Qiagen, Hilden, Germany). Concentration and purity were quantified with a Nanodrop. One µg of RNA was used for reverse transcription with M-MLV reverse transcriptase (Promega, Madison, WI, USA).

For quantitative reverse transcription-polymerase chain reaction (RT-qPCR), protocols were as described before (36). Duplicates were run for each sample. The results were analyzed according to the  $\Delta\Delta Cq$  method (37). *Hprt* was used as the reference gene, and the control group was CHOW fed, HFD fed, or PTU CTRL groups. The numbers of mice used for each experiment are reported in each figure legend. All the primer sequences are listed in Supplementary Table S1 (33).

More details on the procedure are provided in supplemental data file S11 (33).

### Western Blot

The proteins were extracted from the hypothalamus in lysis buffer (50mM Tris-HCl, 10mM EGTA, 1mM EDTA, 16mM Triton X-100, 1mM sodium orthovanadate, 50mM sodium fluoride, 10mM sodium pyrophosphate, and 250mM sucrose). Western blots were transferred to PVDF membranes (PVDF; Millipore; Billerica, MA, USA) and probed with antibodies against pACC $\alpha$  (Ser79) (Cell Signaling Cat# 3661; RRID: AB\_330337; Danvers, MA, USA), pAMPK $\alpha$  (Thr172) (Cell Signaling Cat# 2535S; RRID: AB\_331250) or  $\beta$ -actin (Sigma-Aldrich Cat# A5316; RRID: AB\_476743; St. Louis, MO, USA) as described (8, 9). Adequate secondary antibody: anti-mouse (Agilent Cat# P0260, RRID: AB\_2636929; Santa Clara, CA, USA) or anti-rabbit (Agilent Cat# P0450, RRID: AB\_2630354) was added. Signal of autoradiographic films was quantified by densitometry using ImageJ-1.33 software (NIH; Bethesda, MD, USA). Values were expressed in relation to  $\beta$ -actin. Data are expressed as a percentage of CTRL vehicle and NTRKO vehicle. Representative images for all proteins are shown with all bands for each picture derived from the same gel, although they may be spliced for clarity (represented by vertical black lines). The pACC $\alpha$  and pAMPK $\alpha$  were assayed in the same membranes, therefore, some of the  $\beta$ -actin bands are common in their representative panels; this has been specified in the appropriate figure legend.

### Plasma Biochemistry

Plasma was assayed on a Cobas 6000 automats for free T3 and free T4 with the Cobas e601module (Roche, ECL analyzers),

### D2 Activity

Hypothalamic block or 50 mg BAT tissue was homogenized in lysis buffer (100 mM sodium phosphate, 2 mM EDTA, 50 mM DTT). D2 activity was measured in fresh homogenates. D2

activity was measured in duplicate using 50  $\mu$ L undiluted homogenate (50–100  $\mu$ g protein) that was incubated for 3 hours (hypothalamus) or 2 hours (BAT) at 37 °C in a final volume of 100  $\mu$ L in the presence of 0.25M sucrose, 1mM PTU (to block D1 activity in the hypothalamus), 500nM of T3 (to block D3 activity in the hypothalamus), 1nM T4, and approximately  $1.10^5$  cpm  $^{125}$ I-T4 (in-house, single labeled tracer according to (38) Wiersinga et al in phosphate-EDTA buffer (PE buffer, 100mM sodium phosphate, 2nM EDTA, pH 7.2). D2 activity was expressed as  $^{125}$ I-fmol released per minute per gram of protein. The assay is based on the protocol previously described by Werneck-de-Castro et al (39).

## Histology, Immunohistochemistry

### Adipose tissues

Fixed adipose tissues were embedded in paraffin. Tissue sections (4  $\mu$ m for BAT; 8  $\mu$ m inguinal WAT (iWAT)) were stained with hematoxylin and eosin (H&E). Rabbit polyclonal antibodies directed against UCP1 (Abcam Cat# ab10983, RRID: AB\_2241462, Cambridge, UK) and tyrosine hydroxylase (Abcam Cat# ab112, RRID: AB\_297840) were diluted in PBS/2.5% goat serum for immuno-histochemistry, (1:400 and 1:750 dilution respectively). Sections were deparaffinized and incubated overnight at 4 °C with a primary antibody. Sections were then incubated with an HRP-labeled anti-rabbit (1:300) (Promega Cat# W4011, RRID: AB\_430833) for 1 hour at room temperature. Peroxidase activity was visualized with diaminobenzidine staining (DAB, D5905 Sigma-Aldrich) and counterstained with hematoxylin. The images were acquired using an AxioObserver Zeiss microscope at a 16 $\times$  magnification. Data were collected and the average intensity of the DAB signal was quantified after color deconvolution was performed to separate the relative contributions of DAB and hematoxylin, using ImageJ software. Background correction was performed using a negative control slide, in which the primary antibody was omitted. Three slides per animal were processed.

### Brain

For neuroanatomy experiments, immunohistochemistry was performed on free-floating brain sections as previously described (30). Brain coronal sections (50  $\mu$ m) were cut with a vibrating microtome (Integraslice 7550 SPDS, Campden Instruments, Loughborough, UK), and stored at –20 °C in cryoprotectant (30% ethylene glycol and 20% glycerol in 10mM PBS) prior to immunohistochemistry.

The following primary antibodies were used: mouse anti-NeuN (1:500) (Merck Millipore Cat# MAB377, RRID: AB\_2298772, Burlington, MA, USA), and rabbit anti-GFAP (1:2000) (Agilent Cat# Z0334, RRID: AB\_10013382). Secondary antibodies were made in donkey (ThermoFisher Scientific, anti-rabbit DyLight 488 Cat# SA5\_10038, RRID: AB\_2556618, anti-mouse DyLight 650 Cat# SA5\_10169, RRID: AB\_25556749) and used at a 1:1000 dilution. Sections were imaged using an inverted confocal microscope (Zeiss LSM 780). ImageJ software was used to estimate the proportion of NeuN+ cells that were also tdTomato+ at different levels of the rostrocaudal hypothalamus.

## Quantification and Statistical Analyzes

For mouse experiments, the data presented represent the average values of different animals from the same genotype given

the same treatment. The number of animals ( $n$ ) used is indicated in the figure legends. For RT-qPCR, each sample was run in duplicate. The error bars represent standard error of the mean, since it is more appropriate than SD when  $n \geq 6$ . Statistical relevance was determined using the one-way ANOVA or the T-Test method as indicated in the figure legends. \* or \$ or £ indicates  $P \leq .05$ , \*\* or \$\$ for  $.005 \leq P \leq 0.05$ , \*\*\* or \$\$\$ for  $.0005 \leq P \leq .005$ , \*\*\*\* or \$\$\$\$ for  $P \leq .0005$  (ns indicates nonsignificant). This method is appropriate since the size of the compared groups is similar and the distribution of the samples normal. Given the variability of the phenotype that we observed, we used  $n \geq 6$  to obtain statistically significant results. For only 2 groups,  $n = 5$ , because the animals died during the experimentation procedures.

## Results

### Generation of Mice With Selective Elimination of T3 Signaling in Neurons

Recombination with the *Cre/LoxP* system was used to generate somatic mutations in the *Thra* and *Thrb* genes. The *Cre3<sup>Tg</sup>*, *Thra<sup>AMI</sup>*, and *Thrb<sup>lox</sup>* alleles were combined to obtain *Cre3<sup>Tg/+</sup>Thra<sup>AMI/+</sup>Thrb<sup>lox/lox</sup>* mice, called NTRKO mice (see “Methods”). These mice are heterozygous for the *Thra<sup>AMI</sup>* mutation and express the TR $\alpha$ 1<sup>L400R</sup> in neurons as a result of *Cre/LoxP* mediated recombination. This mutant receptor exerts a dominant-negative activity toward the remaining intact TR $\alpha$ 1 receptor. As mice are also homozygous for a *Thrb* floxed allele, *Cre/LoxP* recombination eliminates the receptors encoded by *Thrb* (27, 28). Therefore, the T3 response is selectively eliminated from all Cre-expressing cells.

The efficacy of Cre-dependent recombination in the *Cre3<sup>Tg</sup>* transgenic mice was first described to be pan-neuronal in both the central and peripheral nervous systems (29). Later studies from our lab showed that the efficiency of recombination was the highest in hypothalamus as compared to other brain areas (30). Here we used a Rosa-tdTomato<sup>lox</sup> reporter (32) to show that Cre activity is merely absent in non-nervous tissues (Supplementary Fig. S1 (33)) and to better evaluate the recombination pattern in the hypothalamus (Supplementary Fig. S2 (33), Fig. 1). The red fluorescence systematically colocalized with the neuronal NeuN marker and did not overlap with the glial marker GFAP (Fig. 1) as previously described in other area of the brain (30). The density of red fluorescent neurons was high in all hypothalamic nuclei (Fig. 1B, Supplementary Fig. S2 (33)), except the suprachiasmatic nucleus (not shown), representing 20% to 42% of all neurons in the counted area (Supplementary Fig. S2 (33)). Therefore, mutations take place in a large fraction of neurons but not in glial cells or other cell types of the brain. We also used TR $\beta$ 1 mRNA level as a marker for Cre-mediated recombination in NTRKO mice and found that it was only decreased in the hypothalamus but not in the peripheral tissues (Fig. 2A). As TRH is produced by the hypothalamic neurons and involved in the feed-back control of TH production by the hypothalamus-pituitary axis, we measured the expression of TRH. In NTRKO TRH levels were unchanged under either CHOW or HFD (Fig. 2B left panel) and repression of TRH by TH in hypothyroid animals was also normal (Fig. 2B right panel). In agreement free T3 and free T4 concentrations in serum were normal in the mutants under all physiological conditions tested in the paper (Supplementary Fig. S3A (33)).

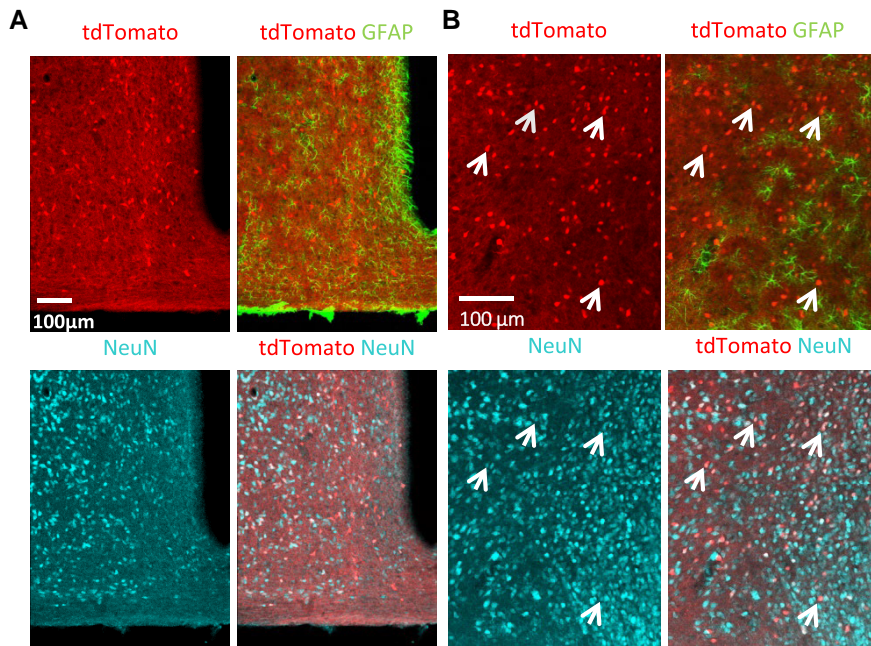


**Figure 1.** Neuron-specific Cre-mediated recombination in the hypothalamus in mice that carry the Cre3 transgene ( $Cre3^{Tg/+}/RosattdTomato^+$  mice). All cells expressing *tdTomato* (Cre-mediated recombination reporter) also expressed NeuN (neuronal marker), while none of them expressed GFAP (glial cell marker). For each field, 4 images of confocal fluorescence microscopy are shown: *tdTomato*, combination of *tdTomato* and GFAP, NeuN, combination of *tdTomato* and NeuN. (A) In the rostral hypothalamus, about 20% of NeuN+ cells also expressed *tdTomato*. (B) In images with higher magnification, which were taken in the dorsomedial hypothalamus, arrows have been added to help verify that all *tdTomato*+ cells were also NeuN+.

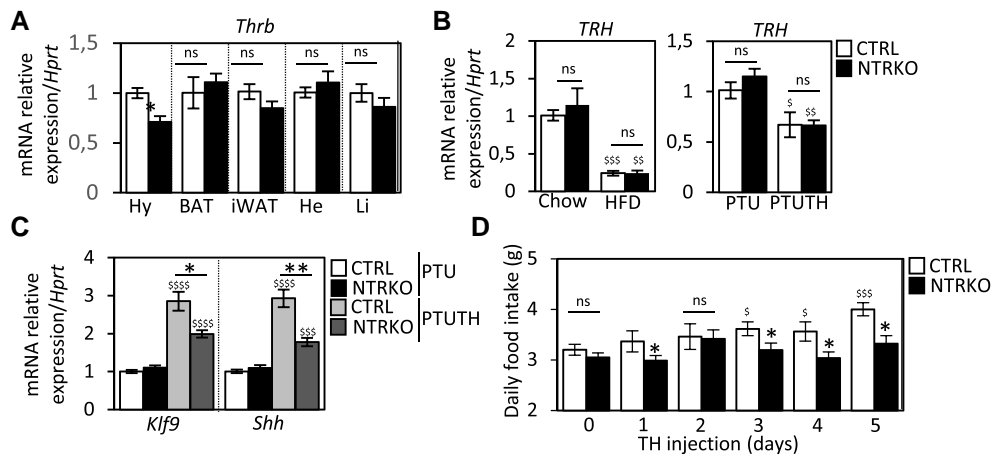


**Figure 2.** Characterization of the NTRKO mice: a model of selective blockade of T3 signaling in neurons. The selective activity of Cre recombinase in the  $Cre3^{Tg}$  transgenic line was evaluated by immunohistochemistry using the  $Cre3^{Tg/+}/RosattdTomato^+$  reporter line (Fig. 1, Supplementary Fig. S1). Different experiments were done to demonstrate neuronal blockade of T3 signaling in NTRKO mice. (A) *Thrb* expression was analyzed by relative RT-qPCR in different tissues of 3- to 4-month-old NTRKO (black  $n = 6$ ) and CTRL (white  $n = 6$ ) males fed a CHOW diet. (B) 6-month-old male mice CTRL or NTRKO fed a CHOW ( $n = 5$  and  $n = 7$ ) or an HFD for 3 months ( $n = 5$  and  $n = 7$ ) (left panel), or 3- to 4-month old males from NTRKO and CTRL rendered hypothyroid by propylthiouracil (PTU) and treated ( $n = 6$  per genotype) or not by T3/T4 (TH) ( $n = 6$  per genotype) (right panel) were sacrificed and hypothalami sampled for RNA preparation. The white and black columns, respectively, represent CTRL and NTRKO. Expression of *TRH* was measured by relative RT-qPCR in the hypothalamus. (C) Expression of well characterized T3 target genes (*Klf9*, *Shh*) was also measured in the hypothalamus of the same PTU/PTUTH treated animals by relative RT-qPCR. CTRL PTU, NTRKO PTU, CTRL PTUTH, and NTRKO PTUTH are, respectively, represented by white, black, light gray, and dark gray bars. (D) 3- to 4-month-old CTRL (white bars  $n = 10$ ) and NTRKO (black bars  $n = 9$ ) male mice were on CHOW diet and injected daily with T3/T4 (TH) for 5 days from D0. Food intake was measured every day. CTRL animals CHOW fed (A, B left panel and D) or PTU fed (B right panel and C) were taken as the reference group. Statistical ANOVA tests were used for pairwise comparisons of CTRL and NTRKO mice. Stars indicated a significant difference between CTRL and mutants in a given condition, dollars a significant difference in a given genotype between 2 conditions. Abbreviation: ns, nonsignificant.

In order to address the capacity of neurons to respond to T3, we treated NTRKO with PTU to make them hypothyroid. In response to TH the expression of the *Sbh* and *Klf9* genes, previously described to be targets of T3 in neurons

(36-40) was blunted in the hypothalamus of the mutants (Fig. 2C). Moreover, whereas administration of TH increased food intake in CTRL mice (41), this response was reduced in the NTRKO mice (Fig. 2D), supporting an

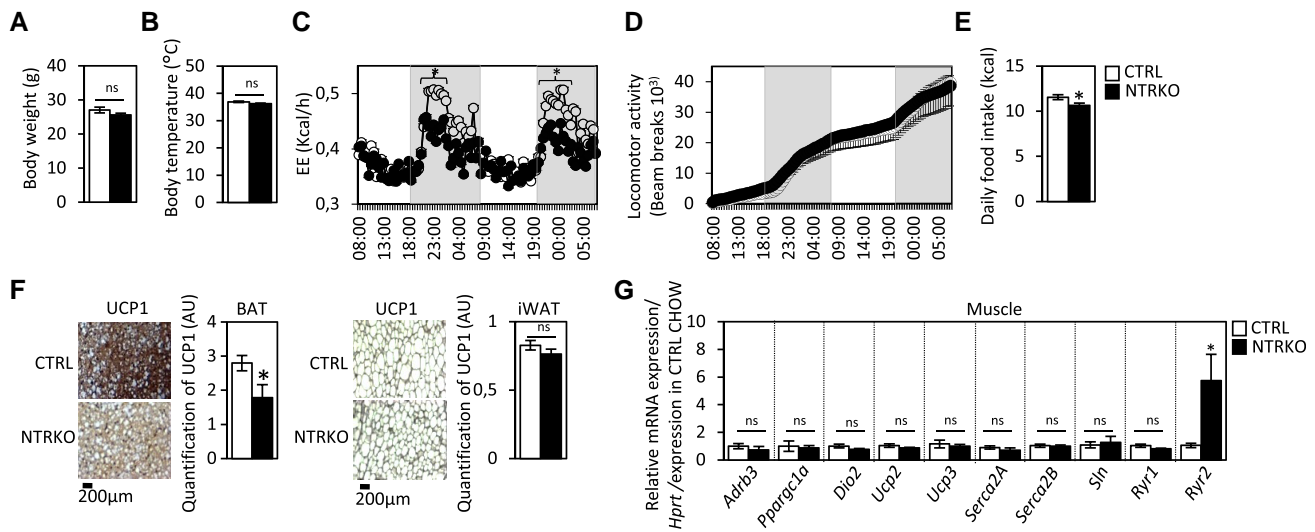


**Figure 3.** T3 signaling in neurons regulates EE. The different metabolic parameters were determined in 4-month-old CTRL ( $n = 12$ ) and NTRKO ( $n = 12$ ) male mice housed at 23°C on a CHOW diet. We measured (A) Body weight (B) Body Temperature (C) EE measured by indirect calorimetry (D), locomotor activity and (E) daily food intake. The gray-shaded areas represent nighttime. (F) Six-month-old male mice CTRL and NTRKO fed a CHOW diet ( $n = 5$  and  $n = 7$ ) at 23°C were sacrificed to sample BAT, iWAT. UCP1 immunostaining was performed on BAT and iWAT slices and quantified by image analysis. (G). The expression of genes involved in nonshivering thermogenesis was measured in the skeletal muscle of the same mice for RT-qPCR. The white and black columns, respectively, represent CTRL and NTRKO. Statistical T-tests were used for pairwise comparisons of CTRL and NTRKO mice in (A, B, C, and D), statistical ANOVA tests for pairwise comparisons of CTRL and NTRKO mice. Abbreviation: ns, nonsignificant.

inactivation of TH signaling in hypothalamic neurons. In contrast, a normal TH response was observed in all peripheral tissues that we tested. This was ascertained by measuring the mRNA levels for *Klf9* and *Hr* in inguinal WAT (iWAT), BAT, and heart, or *Hr* and *Thrsp* in liver (Supplementary Fig. S3B (33)).

In summary, NTRKO mice are euthyroid with functional T3 signaling in all cell types except for a fraction of neurons.

### T3 Signaling in Neurons Regulates EE

The NTRKO phenotype was first analyzed under standard conditions of food and temperature. Their body weight (Fig. 3A) and temperature (Fig. 3B) were normal. Their EE (Fig. 3C) measured by indirect calorimetry was lower than that of CTRL mice. Their locomotor activity (Fig. 3D) was similar, but NTRKO food intake (Fig. 3E) was slightly lower. RT-qPCR analyses did not reveal any major alteration of neither the thermogenic program in BAT (*Dio2*, *Ucp1*, *mCCKB*, and *mAlpl* mRNA) (Supplementary Fig. S4A (33)) nor the browning program in iWAT (*Ppargc1a*, *Ucp1*, *Cidea*, *Cox7c*, and *Prdm6*) (Supplementary Fig. S4B (33)). However, UCP1 protein level was lower in BAT of NTRKO mice (Fig. 3F). We also assessed UCP1-independent nonshivering thermogenesis in skeletal muscle, by measuring the expression of the genes involved in  $Ca^{2+}$  cycling (*Serca2A*, *Serca2B*, *Sln*, *Ryr1*, *Ryr2*) (18). We found an increase in *Ryr2* expression in NTRKO muscles (Fig. 3G). Thermogenic mechanisms might be turned on in muscle to compensate defective BAT activity.

### T3 Signaling in Neurons is not Involved in Severe Cold-induced Thermogenesis

As increased D2 activity and local production of T3 in the BAT are critical to the cold response in wild-type mice (WT) (21), the activity of D2 was checked in the hypothalamus of WT mice. It was not modified during cold exposure in the

hypothalamus but, as expected, was strongly induced in the BAT (Fig. 4A).

To test whether despite the unchanged D2 activity in hypothalamus, impaired T3 signaling in neurons prevents the cold-induced process of adaptive thermogenesis, mice were exposed to 4 °C. Their body weight (Fig. 4B) and body temperature (Fig. 4C) were monitored for 2.5 days. Both NTRKO and CTRL mice managed to maintain their body temperature by increasing their food intake (Fig. 4D). Thermogenesis of BAT was observed by infrared thermography after 24 and 48 hours at 4 °C. The temperature of this tissue was similar in the 2 genotypes at both time points (Supplementary Fig. S5A (33)). Accordingly, the UCP1 protein was expressed at the same level in NTRKO and CTRL in both BAT (Fig. 4E) and in iWAT (Supplementary Fig. S5B (33)) at 4 °C. Moreover RT-qPCR analyses did not reveal any major alteration of either the thermogenic program in BAT (*Dio2*, *Ucp1*, *mCCKB*, and *mAlpl* mRNA) (Fig. 4E) or the browning program in iWAT (*Ppargc1a*, *Ucp1*, *Cidea*, *Cox7c*, and *Prdm6*) at this temperature (Supplementary Fig. S5B (33)).

The general response of BAT tissue to SNS stimulation, estimated by the level of expression of *Dio2*, *Ucp1*, and *Elavl6*, is similar in the NTRKO BAT at 4 °C compared to CTRL (Fig. 4F). However, the expression of the *Adrb3* gene encoding the adrenergic receptor beta 3 the main sensor in BAT for cold-triggered SNS activation, and of one of the genes upregulated after this activation (*Ppargc1a*) were higher in the NTRKO BAT under the same condition. A possible interpretation of these results would be that a slight increase in BAT sensitivity to SNS stimulation allows NTRKO mice to face a cold challenge.

### Inhibition of T3 Signaling in Neurons Alters the Response to DIO

When fed an HFD, NTRKO mice gained more weight than CTRL (Fig. 5A). This resulted from higher body fat accumulation (Fig. 5B) without any significant changes in food intake

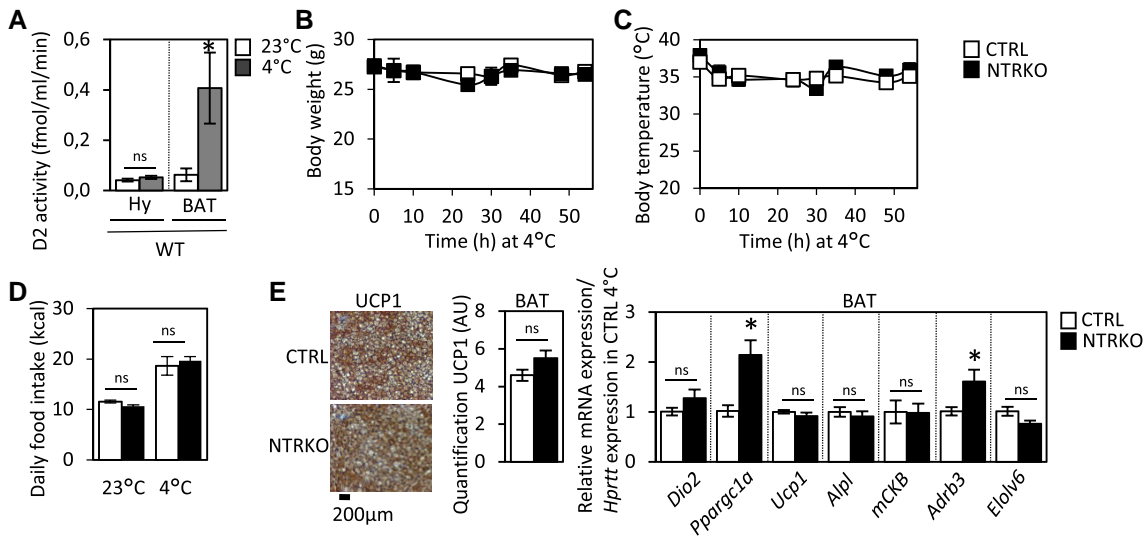


**Figure 4.** Blocking T3 signaling in neurons does not affect cold-induced thermogenesis. (A) D2 activity was assayed in hypothalamus (Hy) and BAT of 2-month-old C57bl6 males maintained for 58 hours at 4 °C ( $n = 6$ ) (gray bars) or 23 °C ( $n = 6$ ) (white bars). Five 4-month-old CTRL ( $n = 6$ ) and NTRKO ( $n = 6$ ) male mice were housed at 4 °C for 58 hours. White and black squares/columns respectively represent CTRL and NTRKO. (B) Body weight, (C) temperature as measured by telemetry, and (D) food intake were measured during cold exposure. BAT was sampled after cold exposure for histology and RT-qPCR analyses. (E) (left panel) UCP1 immunostaining was performed on BAT slices and quantified by image analysis. Markers of  $\beta$  adrenergic response/BAT activity in the BAT were analyzed by relative RT-qPCR (right panel). Statistical ANOVA tests were used for pairwise comparisons of 2 temperatures in a given organ in (A), of CTRL and NTRKO mice in (B, C, D, E). Abbreviation: ns, nonsignificant.

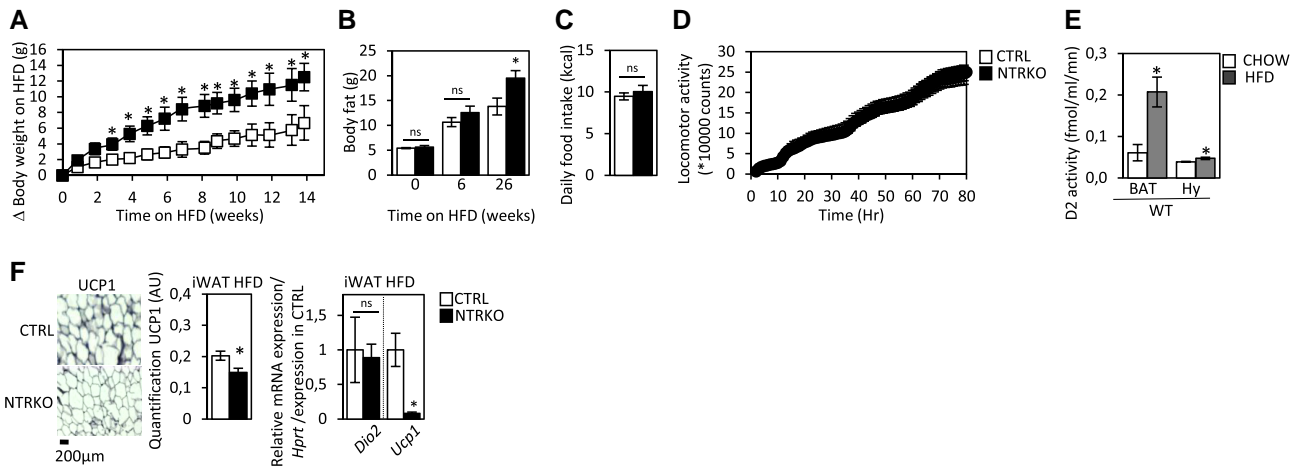


**Figure 5.** Blocking T3 signaling in neurons prevents adequate response to diet-induced obesity (DIO). CTRL ( $n = 9$ ) and NTRKO ( $n = 9$ ) male mice (2- to 3-months old) were fed a CHOW diet and then switched to an HFD (time 0). Their body weight was measured once a week. (A) Body weight gain ( $\Delta$  body weight) was calculated between any time point and the day diet was switched to HFD. (B) Body fat mass was evaluated by echoMRI at 3 time points. (C) Daily food intake was measured and locomotion (D) was studied for 4 consecutive days on HFD. (E) D2 activity was measured in the BAT and hypothalamus (Hy) of 2-month-old C57bl6 mice fed either a CHOW diet ( $n = 5$ ) or an HFD ( $n = 6$ ) for 3.5 days. Tissues were sampled from 6-month-old male mice either CTRL or NTRKO fed an HFD for 3 months ( $n = 5$  and  $n = 7$ ). (F) iWATs were used for histology or RNA preparation. UCP1 immunostaining was performed on iWAT slices (left panel). The expression of markers of browning in iWAT (right panel) were assessed by relative RT-qPCR. The white and black columns, respectively, represent CTRL and NTRKO. CTRL animals were taken as the reference group. Statistical T-tests were used for pairwise comparisons of CTRL and NTRKO mice in (A, B, C, and D). Statistical ANOVA tests were used for pairwise comparisons of 2 temperatures in a given organ in (E), of CTRL and NTRKO mice in (F). C, D, E). Abbreviation: ns, nonsignificant.

(Fig. 5C) or locomotor activity (Fig. 5D). Circulating levels of total cholesterol and triglycerides were regulated on HFD to a similar extent in both genotypes (Supplementary Fig. S3C (33)). In WT animals, D2 enzymatic activity in the hypothalamus increased slightly but significantly after 3.5 days of HFD (Fig. 5E). To characterize the altered response of mutant mice to DIO, we measured gene expression in the BAT of NTRKO and CTRL mice after an HFD. The expression of genes

involved in the thermogenic program or the response to SNS stimulation and the level of UCP1 protein were not affected (Supplementary Fig. S6A (33)). The gene expression analysis in muscle did not provide an indication of a defect in nonshivering thermogenesis in NTRKO mice (Supplementary Fig. S6B (33)). By contrast, quantification of *Ucp1* mRNA and UCP1 protein (Fig. 5F) in iWAT showed that browning was less efficient in the mutants under HFD. Therefore, an impairment in

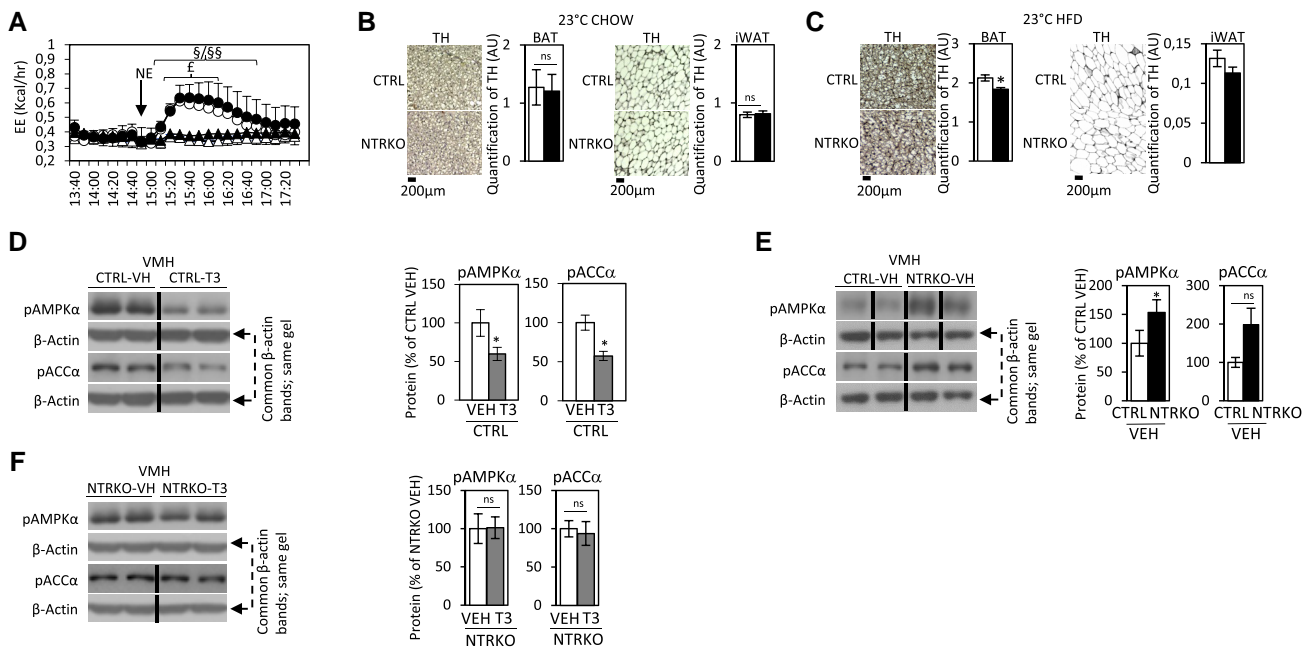


**Figure 6.** Neuron T3 signaling interferes with SNS signaling to regulate EE. CTRL and NTRKO male mice (4 months old) were injected (6 per genotype) (squares) or not (circles) with norepinephrine (NE) ( $n=6$  per genotype) at the time marked by an arrow. (A) EE was recorded by indirect calorimetry before and after injection Tyrosine Hydroxylase is expressed in nerve endings and catalyzes the production of NE. TH immunostaining was performed and quantified on BAT (left panels) and iWAT (right panels) isolated from (B) CHOW-fed ( $n=5$  for CTRL and  $n=7$  for NTRKO) or (C) HFD-fed ( $n=9$  of each genotype) CTRL or NTRKO 6-month-old male mice housed at 23 °C. CTRL and NTRKO male mice (4 months old) were ICV injected with T3 ( $n=6$  per genotype) or vehicle (VEH) ( $n=6$  per genotype). After dissection, proteins were extracted from VMH and the quantity of pAMPK $\alpha$  and pACC $\alpha$  estimated by Western blot.  $\beta$ -actin is used for normalization. (D/E/F) Blots are provided on the left, (D/E/F) their quantification on the right. The previously described effect of T3 in CTRL is depicted in (D), the effect of the mutation is in (E), and the lack of effect of T3 in NTRKO in (F). In the Western blot analyses, values were expressed in relation to  $\beta$ -actin. Representative images for all proteins are shown; all the bands for each picture are derived from the same gel, although they may be spliced for clarity (represented by vertical black lines). pAMPK $\alpha$  and pACC $\alpha$  were assayed in the same membranes, therefore, some of the  $\beta$ -actin bands are common in their representative panels, this has been specified in Fig. 6D-6F. (A, D, E, and F) Statistical T-tests or (B, C) Statistical ANOVA tests were used for pairwise comparisons in (B, C, E) of CTRL and NTRKO mice, in (A) of CTRL NE and CTRL (§) and of NTRKO NE and NTRKO, in (D) of CTRL T3 and CTRL VEH and in (F) of NTRKO T3 and NTRKO VEH. Abbreviation: ns, nonsignificant.

iWAT browning might explain the observed sensitivity to DIO (Fig. 5A).

### Neuronal T3 Signaling Modulates SNS Signaling to Regulate EE

Inefficient browning of iWAT under HFD, increased expression of the *Adrb3* gene in BAT at 4 °C, and decreased levels of UCP1 protein in both BAT and iWAT under different conditions, all point to possible inadequate SNS signaling in NTRKO mutants. We housed mice at 30 °C, to address the sensitivity of mutant mice to DIO in the absence of thermogenic SNS stimulation (42). In this condition, obesity was more pronounced in CTRL mice than at 23 °C ( $\Delta$ body weight after 12 weeks of HFD, 9 g vs 5 g at 23 °C). Most importantly, the difference between mutant and control mice disappeared at 30 °C (Supplementary Fig. S7A (33)). The level of UCP1 protein in BAT was similar in both genotypes under the CHOW diet (Supplementary Fig. S7B (33)) in contrast to what was observed at 23 °C. Normalization of the NTRKO phenotype at thermoneutrality provides a strong argument suggesting that the sensitivity of NTRKO to DIO at 23 °C originates from a defect in the tone of the SNS. To address the alternative possibility, which would be that mutant thermogenic organs are less sensitive to SNS stimulation, we treated NTRKO and CTRL mice with NE to activate  $\beta$  adrenergic receptor in BAT and measured the induced change in EE (Fig. 6A). Mutant and control mice responded equally well to

this stimulation, reinforcing our initial interpretation. This was further reinforced by performing tyrosine hydroxylase immunostaining in BAT and iWAT, which allows us to indirectly assess the autonomic nervous input and adrenergic signaling on both CHOW (Fig. 6B) and HFD (Fig. 6C) (43). This revealed a slight alteration in the capacity of NTRKO mice to produce catecholamines on HFD (Fig. 6C).

We then assessed more directly the capacity of the hypothalamus to respond to a local T3 stimulation by performing intracerebroventricular (ICV) injections of T3 (Fig. 6D-6F). This treatment reduced AMPK and acetyl-coA carboxylase (ACC) phosphorylation levels in the hypothalamus of CTRL mice, as previously described (9, 10, 44) (Fig. 6D). Notably, the steady-state levels of pAMPK $\alpha$  and pACC $\alpha$  was higher in NTRKO ventromedial hypothalamus (VMH) than in the VMH of CTRL mice (Fig. 6E) and was not decreased after local T3 injection (Fig. 6F). This supports the inhibitory effect of T3 on AMPK signaling and the requirement for functional TR in neuron to mediate this response.

### Discussion

Data published in recent years provided distinct but complementary pieces of information on the mechanisms by which exogenous T3 influences energy homeostasis (9-11, 44, 45). ICV or intra-VMH injection of T3 for short term or up to 28 days increases SNS tone, BAT activity, and EE (9, 10, 44). Despite increased UCP1 expression in BAT and iWAT,

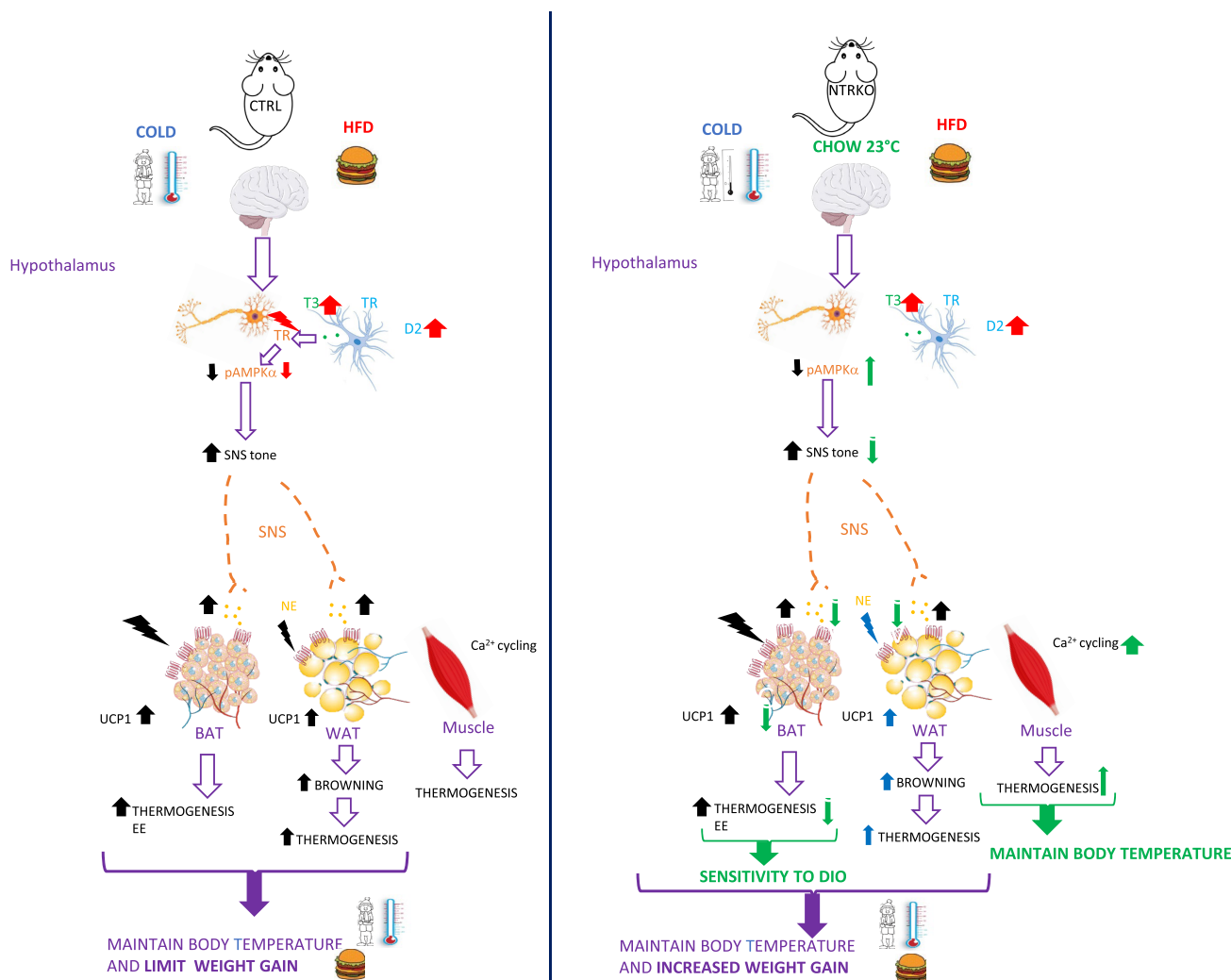


**Figure 7.** Proposed model for the role of T3 in neurons for regulation of energy expenditure in response to cold and HFD. On the left panel, a scheme of regulation of energy expenditure in response to cold and HFD in CTRL mice. Black arrows picture the regulation observed under either COLD or HFD stimuli as compared respectively to 23 °C and CHOW diet (the amplitude of the response might be different under cold and HFD). The Blue arrows the regulation observed only at 4 °C, the red the regulation observed only under HFD. The lightning sign stands for activation. On the right panel are summarized 3 situations in the NTRKO. In green it shows, the difference of energy regulation pathways in the NTRKO as compared to CTRL on regular conditions (CHOW and 23 °C). Black arrows picture the regulation observed in NTRKO under either COLD or HFD as compared respectively to 23 °C and CHOW diet. Red arrows picture the regulation observed only under HFD as compared to CHOW in the NTRKO and the Blue arrows the regulation only observed at 4 °C as compared to 23 °C in NTRKO as well.

systemic hyperthyroidism increases EE also via the activation of thermogenic mechanisms in the muscle (8, 46). Our study provides strong genetic support to previous hypotheses drawn from these experiments and sheds light on the importance of endogenous T3 signaling in neurons in facing thermogenic stresses.

Here we generated NTRKO, a new mouse model in which Cre-mediated mutations of TR in neurons induce a selective blockade of T3 signaling in these neurons. In a previous study, using the same Cre (*Cre3<sup>Tg/+</sup>Thra<sup>AMU/+</sup>*) Richard et al (30). described that the expression of hairless (*Hr*), a T3 target gene, was deregulated in hypothalamus but not in other cerebral areas such as the hippocampus, the cortex, and the cerebellum. The hypothalamus must be one of the brain areas that is the most impacted by the mutations. Here we show that the decrease of *Thrb* expression was only observed in the hypothalamus and not in peripheral tissues. This decrease was only partial, since *Thrb* is also

expressed in glia and only 20% to 42% of neurons express Cre. However, it was sufficient to observe a significant decrease of *Shb* and *Klf9* expression, 2 well-described T3 target genes, in response to T3. Importantly, the circulating levels of TH in NTRKO mice are similar to CTRL in all physiological conditions tested and so is the regulation of *TRH* expression by TH. This suggests that TR are still functional in TRH-expressing neurons to repress *TRH* expression in response to TH and that regulation of the hypothalamo-pituitary-thyroid axis by TH remains unaltered in NTRKO mice. Altogether these mice are euthyroid with functional T3 signaling in all cell types except for a fraction of neurons mainly in hypothalamus.

Selective blockade of T3 signaling in NTRKO neurons triggers a decrease in EE that mirrors the increase of EE previously described after T3 injection in the hypothalamus. Our data suggest that EE is altered in NTRKO as a result of decreased uncoupling of catabolism and ATP production in BAT. Calcium

futile cycling in myotubes might produce heat at 23 °C to compensate for the BAT defect and to maintain normal body temperature in NTRKO mice under this mild cold stress.

Importantly, our data show that endogenous T3 signaling in neurons is mainly relevant for an adequate response to HFD, as NTRKO manage to maintain body temperature after a cold challenge.

D2 activity is increased in the hypothalamus in response to HFD but not cold. That suggests that the local production of T3 in the hypothalamus does not change during cold exposure and that the neuronal response to T3 is not recruited for cold-induced adaptive thermogenesis. In contrast local production of T3 in the hypothalamus would increase under HFD and the inability of NTRKO to properly detect intrahypothalamic production of T3 would be responsible for their higher sensitivity to DIO.

Interaction with the SNS is involved in the NTRKO sensitivity to DIO, as it is normalized at thermoneutrality. Modulation of the hypothalamic AMPK pathway plays an important role in the central action of T3 on both BAT and liver metabolism (9, 10, 44). Our data show that while central T3 decreases pAMPK $\alpha$  and pACC $\alpha$  protein levels, the absence of T3 signaling in neurons increases the basal level of these 2 phosphoproteins and blunts their regulation by T3. The expected result is a reduced SNS tone to BAT in NTRKO mice at 23 °C on CHOW diet. Consequently, under these conditions the level of UCP1 protein in BAT is reduced. The associated decreased in BAT activity might be responsible for the decrease in EE and could be compensated by alternative thermogenic mechanisms, which include the activation of the Ca<sup>2+</sup> futile cycle in the skeletal muscle to maintain body temperature of NTRKO at 23 °C. In any case, these results confirm that T3-induced thermogenesis in the brain mostly relies on stimulation of the BAT, while peripheral T3 administration also stimulates not only BAT (6) but also muscle thermogenesis (8, 46).

Thus, T3 signaling in neurons is an important player in the regulation of EE. The interference with the AMPK regulation for SNS activation, previously described after central administration of T3, appears to be also relevant when a physiological thermogenic stress stimulates the hypothalamic production of T3. Importantly NTRKO mice efficiently maintained their body temperature when exposed to an intense cold, displaying normal BAT and WAT response, despite a suboptimal SNS tone. We propose a model for the role played by T3 in neurons for the regulation of EE in response to cold and HFD in Fig. 7.

This contrasts with data obtained in a mouse model that ubiquitously expressed TR $\alpha$ 1<sup>R384C</sup> another dominant negative TR $\alpha$ 1 (47). Unlike NTRKO, these mice are hypermetabolic and hypothermic, with a theoretical defended temperature of 38 °C (48). In-depth phenotyping led to the conclusions that this phenotype is primarily due to a chronic vasodilatation, which increases heat dissipation. The defect in vasoconstriction was found to reflect a reduced sensitivity of blood vessels to SNS stimulation (49) that should not take place in NTRKO mice.

## Conclusions

We show that T3 does control EE under physiological stresses via its action in neurons. Moreover, although selective inhibition of T3 signaling in neurons leads to a less severe metabolic phenotype than hypothyroidism, modulation of T3

concentration and signaling in neurons definitively represents a significant fraction of metabolic regulation by T3. Targeting T3 to neurons in adult might help fight obesity.

## Limitations to Our Study

First, the Cre-induced mutations occur in juveniles and are not restricted to adult life. Therefore, we cannot rule out that the postnatal maturation of neuronal circuits is altered in mutant mice; even so, we did not observe any obvious behavioral abnormality. Similarly, while the hypothalamus is the area of the brain that displays the highest percentage of Cre-mediated recombination and that is known to control EE, the intervention of other brain areas in the determination of the metabolic phenotype of NTRKO is possible. Finally, only male mice were included in the study. Since sex specificity can occur in metabolic responses, similar experiments should be run on females.

Further analyzes using models with selective inhibition of T3 signaling in other metabolic tissues, specific neuronal populations, and other brain cell types would clarify the mechanism by which T3 regulates energy balance.

## Acknowledgments

We thank Andres del Valle who contributed with RT-qPCR analyzes; Nadine Aguilera, Marie Teixeira, and the ANIRA-PBES facility for help in transgenesis and mouse breeding; Catherine Cerrutti and the members of the Flamant Lab for fruitful discussions and Marja van Veen for her technical help.

## Funding

This work was supported by grants from the French ANR (FF Thyromut2 program; ANR-15-CE14-0011-01); from ANSES (Thyrogenox); from Ministerio de Ciencia e Innovación cofunded by the EU FEDER Program (ML: PID2021-128145NB-I00) and “la Caixa” Foundation (ID 100010434), under the agreement LCF/PR/HR19/52160022. ER-P was recipient of a fellowship from MINECO (BES-2015-072743). CC is supported by the Lundbeck Foundation (Fellowship R238-2016-2859) and the Novo Nordisk Foundation (grant number NNF17OC0026114). TDM received funding from the German Research Foundation (DFG TRR296, TRR152, SFB1123 and GRK 2816/1), the German Center for Diabetes Research (DZD e.V.) and the European Research Council ERC-CoG Trusted no. 101044445.

## Author Contributions

K.G., F.F., and M.L. conceived the study. K.G., E.R.-P., and C.C. ran the in vivo experiments. T.D.M. participated in study design and interpretation of data. L.C. ran the thermography experiments, and performed the histology/immune histology studies, S.W. performed some immune histology studies, J.W. and A.B. measured D2 activity. E.R.-P., K.G., R.G., and S.R. performed in vitro experiments. K.G., F.F., and M.L. wrote the paper. All authors helped analyze the data and reviewed and commented on the final manuscript.

## Disclosures

We declare no competing interest.

## Data Availability

Original data generated and analyzed during this study are included in this published article or in the data repository listed in the references (<https://doi.org/10.6084/m9.figshare.22047992>).

## References

- Blüher M. Obesity: global epidemiology and pathogenesis. *Nat Rev Endocrinol.* 2019;15(5):288-298.
- Zekri Y, Flamant F, Gauthier K. Central vs. peripheral action of thyroid hormone in adaptive thermogenesis: a burning topic. *Cells.* 2021;10(6):1327.
- Cicatiello AG, Di Girolamo D, Dentice M. Metabolic effects of intracellular regulation of thyroid hormone: old players, new concepts. *Front Endocrinol.* 2018;9:474.
- Chouchani ET, Kazak LL, Spiegelman BM. New advances in adaptive thermogenesis: UCP1 and beyond. *Cell Metab.* 2019;29(1):27-37.
- Golozoubova V, Cannon B, Nedergaard J. UCP1 Is essential for adaptive adrenergic nonshivering thermogenesis. *Am J Physiol Endocrinol Metab.* 2006;291(2):E350-E357.
- Zekri Y, Guyot R, Suárez IG, et al. Brown adipocytes local response to thyroid hormone is required for adaptive thermogenesis in adult male mice. *Elife.* 2022;11:e81996.
- Obregon MJ. Adipose tissues and thyroid hormones. *Front Physiol.* 2014;5:479.
- Nicolaisen TS, Klein AB, Dmytriyeva O, et al. Thyroid hormone receptor alpha in skeletal muscle is essential for T3-mediated increase in energy expenditure. *FASEB J.* 2020;34(11):15480-15491.
- Martinez-Sánchez N, Moreno-Navarrete JM, Contreras C, et al. Thyroid hormones induce the browning of white fat. *J Endocrinol.* 2017;232(2):351-362.
- López M, Varela L, Vázquez MJ, et al. Hypothalamic AMPK and fatty acid metabolism mediate thyroid regulation of energy balance. *Nat Med.* 2010;16(9):1001-1008.
- Capelli V, Diéguez C, Mittag J, López M. Thyroid wars: the rise of central actions. *Trends Endocrinol Metab.* 2021;32(9):659-671.
- Cannon B, Nedergaard J. Brown adipose tissue: function and physiological significance. *Physiol Rev.* 2004;84(1):277-359.
- Fliers E, Klieverik LP, Kalsbeek A. Novel neural pathways for metabolic effects of thyroid hormone. *Trends Endocrinol Metab.* 2010;21(4):230-236.
- López M, Alvarez CV, Nogueiras R, Diéguez C. Regulation of energy balance by thyroid hormones at central level. *Trends Mol Med.* 2013;19(7):418-427.
- Kazak L, Chouchani ET, Jedrychowski MP, et al. A creatine-driven substrate cycle enhances energy expenditure and thermogenesis in beige fat. *Cell.* 2015;163(3):643-655.
- Rahbani JF, Roesler A, Hussain MF, Samborska B, Dykstra CB, Tsai L. Creatine kinase B controls futile creatine cycling in thermogenic fat. *Nature.* 2021;590(7846):480-485.
- Sun Y, Rahbani JF, Jedrychowski MP, et al. Mitochondrial TNAP controls thermogenesis by hydrolysis of phosphocreatine. *Nature.* 2021;593(7860):580-585.
- Bal NC, Sahoo SK, Maurya SK, Periasamy M. The role of sarcolipin in muscle nonshivering thermogenesis. *Front Physiol.* 2018;9:1217.
- Saito M, Matsushita M, Yoneshiro T, Okamatsu-Ogura Y. Brown adipose tissue, diet-induced thermogenesis, and thermogenic food ingredients: from mice to men. *Front Endocrinol.* 2020;11:222.
- Kozak LP. Brown fat and the myth of diet-induced thermogenesis. *Cell Metab.* 2020;11(4):263-267.
- de Jesus LA, Carvalho SD, Ribeiro MO, et al. The type 2 iodothyronine deiodinase is essential for adaptive thermogenesis in brown adipose tissue. *J Clin Invest.* 2001;108(9):1379-1385.
- Castillo M, Hall JA, Correa-Medina M, et al. Disruption of thyroid hormone activation in type 2 deiodinase knockout mice causes obesity with glucose intolerance and liver steatosis only at thermoneutrality. *Diabetes.* 2011;60(4):1082-1089.
- Guadaño-Ferraz A, Obregon MJ, St. Germain DL, Bernal J. Type 2 iodothyronine deiodinase is expressed primarily in glial cells in the neonatal rat brain. *PNAS.* 1997;94(19):10391-10396.
- Samarut J, Plateroti M. Thyroid hormone receptors: several players for one hormone and multiple functions. *Methods Mol Biol.* 2018;1801:1-8.
- Martinez-Sánchez N, Seoane-Collazo P, Contreras C, et al. Hypothalamic AMPK-ER stress-JNK1 axis mediates the central actions of thyroid hormones on energy balance. *Cell Metab.* 2017;26(1):212-229.
- Roh E, Kim MS. Brain regulation of energy metabolism. *Endocrinol Metab (Seoul).* 2016;31(4):519-524.
- Quignodon L, Vincent S, Winter H, Samarut J, Flamant F. A point mutation in the 2 domain of thyroid hormone receptor alpha1 expressed after CRE-mediated recombination partially recapitulates hypothyroidism. *Mol Endocrinol.* 2007;21(10):2350-2360.
- Winter H, Rüttiger L, Müller M, et al. Deafness in TRbeta mutants is caused by malformation of the tectorial membrane. *J Neurosci.* 2009;29(8):2581-2587.
- Banares S, Zeh K, Krajewska M, et al. Novel pan neuronal Cre transgenic line for conditional ablation of genes in the nervous system. *Genesis.* 2005;42(1):6-16.
- Richard S, Aguilera N, Thévenet M, Dkhissi-Benyahya O, Flamant F. Neuronal expression of a thyroid hormone receptor  $\alpha$  mutation alters mouse behavior. *Behav Brain Res.* 2017;321:18-27.
- Srinivas S, Watanabe T, Lin CS, et al. Cre reporter strains produced by the targeted insertion of EYFP and ECFP into the ROSA26 locus. *BMC Dev Biol.* 2001;1(1):4.
- Madisen L, Zwingman TA, Sunkin SM, et al. A robust and high-throughput cre reporting and characterization system for the whole mouse brain. *Nat Neurosci.* 2010;13(1):133-140.
- Rial-Pensado E, Canaple L, Guyot R, Clemmensen C, Wiersema J, Wu S. ERP supplemental data file. doi:10.6084/m9.figshare.22047992
- Weiss RE, Murata Y, Cua K, Hayashi Y, Seo H, Refetoff S. Thyroid hormone action on liver, heart, and energy expenditure in thyroid hormone receptor beta-deficient mice. *Endocrinology.* 1998;139(12):4945-4952. Erratum in: *Endocrinology.* 2000;141(12):4767.
- Imbernon M, Beiroa D, Vázquez MJ, et al. Central melanin-concentrating hormone influences liver and adipose metabolism through specific hypothalamic nuclei and efferent autonomic/JNK1 pathways. *Gastroenterology.* 2013;144(3):636-649.e6.
- Chatonnet F, Guyot R, Benoît G, Flamant F. Genome-wide analysis of thyroid hormone receptors shared and specific functions in neural cells. *Proc Natl Acad Sci U S A.* 2013;110(8):E766-E775.
- Bookout AL, Mangelsdorf DJ. Quantitative real-time PCR protocol for analysis of nuclear receptor signaling pathways. *Nucl Recept Signal.* 2003;1(1):e012.
- Wiersinga WM, Chopra IJ. Radioimmunoassay of thyroxine (T4), 3,5,3'-triiodothyronine (T3), 3,3',5'-triiodothyronine (reverse T3, rT3) and 3,3'-diiodothyronine (T2). *Methods Enzymol.* 1982;84:272-303.
- Werneck-de-Castro JP, Fonseca TL, Ignacio DL, et al. Thyroid hormone signaling in male mouse skeletal muscle is largely independent of D2 in myocytes. *Endocrinology.* 2015;156(10):3842-3852.
- Desouza LA, Sathanoori M, Kapoor R, et al. Thyroid hormone regulates the expression of the sonic hedgehog signaling pathway in the embryonic and adult Mammalian brain. *Endocrinology.* 2011;152(5):1989-2000.
- Kong WM, Martin NM, Smith KL, et al. Triiodothyronine stimulates food intake via the hypothalamic ventromedial nucleus independent of changes in energy expenditure. *Endocrinology.* 2004;145(11):5252-5258.
- Ganeshan K, Chawla A. Warming the mouse to model human diseases. *Nat Rev Endocrinol.* 2017;13(8):458-465.
- de Matteis R, Ricquier D, Cinti S. Immunoreactive nerves of TH, NPY, SP, and CGRP in interscapular brown adipose tissue of adult rats acclimated to different temperatures: an immunohistochemical study. *J Neurocytol.* 1998;27(12):877-886.

44. Alvarez-Crespo M, Csikasz RI, Martínez-Sánchez N, *et al.* Essential role of UCP1 in modulating the central effects of thyroid hormones on energy balance. *Mol Metab.* 2016;5(4):271-282.
45. Zhang Z, Foppen E, Su Y. Metabolic effects of chronic T<sub>3</sub> administration in the hypothalamic paraventricular and ventromedial nucleus in male rats. *Endocrinology.* 2016;157(10):4076-4085.
46. Johann K, Cremer AL, Fischer AW, *et al.* Thyroid hormone-induced browning of white adipose tissue does not contribute to thermogenesis and glucose consumption. *Cell Rep.* 2019;27(11):3385-3400.e3.
47. Tinnikov A, Nordström K, Thorén P, *et al.* Retardation of post-natal development caused by a negatively acting thyroid hormone receptor alpha1. *EMBO J.* 2002;21(19):5079-5087.
48. Sjögren M, Alkemade A, Mittag J, *et al.* Hypermetabolism in mice caused by the central action of an unliganded thyroid hormone receptor alpha1. *EMBO J.* 2007;26(21):4535-4545.
49. Warner A, Rahman A, Solsjö P, *et al.* Inappropriate heat dissipation ignites brown fat thermogenesis in mice with a mutant thyroid hormone receptor  $\alpha$ 1. *Proc Natl Acad Sci U S A.* 2013;110(40):16241-6.